Available online at www.sciencedirect.com

ScienceDirect

Energy Procedia 45 (2014) 1392 – 1401

Energy Procedia

68th Conference of the Italian Thermal Machines Engineering Association, ATI2013

Modelling of Thermoacoustic Combustion Instabilities Phenomena: Application to an Experimental Test Rig

Davide Laera[a,*], Giovanni Campa[a], Sergio M. Camporeale[a], Edoardo Bertolotto[b], Sergio Rizzo[b], Federico Bonzani[b], Antonio Ferrante[c], Alessandro Saponaro[c]

[a]*Dipartimento di Meccanica, Matematica e Management - Politecnico di Bari, Via Re David 200, 70125 Bari, Italy*
[b]*Ansaldo Energia spa, Via Nicola Lorenzi 8, 16152 Genova (GE), Italy*
[c]*Centro Combustione Ambiente srl, Via Milano km 1.600, 70023 Gioia del Colle (BA), Italy*

Abstract

Lean premixed combustion chambers fuelled by natural gas and used in modern gas turbines for power generation are often affected by combustion instabilities generated by mutual interactions between pressure fluctuations and heat oscillations produced by the flame. Due to propagation and reflection of the acoustic waves in the combustion chamber, very strong pressure oscillations are generated and the chamber may be damaged. This phenomenon is generally referred as *thermoacoustic instability*, or *humming*, owing to the cited coupling mechanism of pressure waves and heat release fluctuations.

Over the years, several different approaches have been developed in order to model this phenomenon and to define a method able to predict the onset of thermoacoustic instabilities. In order to validate analytical and numerical thermoacoustic models, experimental data are required. In this context, an experimental test rig is designed and operated in order to characterize the propensity of the burner to determine thermoacoustic instabilities.

In this paper, a method able to predict the onset of thermoacoustic instabilities is examined and applied to a test rig in order to validate the proposed methodology. The experimental test is designed to evaluate the propensity to thermoacoustic instabilities of full scale Ansaldo Energia burners used in gas turbine systems for production of energy.

The experimental work is conducted in collaboration with Ansaldo Energia and CCA (Centro Combustione e Ambiente) at the Ansaldo Caldaie facility in Gioia del Colle (Italy).

Under the hypotheses of low Mach number approximation and linear behaviour of the acoustic waves, the heat release fluctuations are introduced in the acoustic equations as source term. In the frequency domain, a complex eigenvalue problem is solved. It allow us to identify the frequencies of thermoacoustic instabilities and the growth rate of the pressure oscillations.

The Burner Transfer Matrix (BTM) approach is used to characterize the influence of the burner characteristics.

Furthermore, the influence of different operative conditions is examined considering temperature gradients along the combustion chamber.

Selection and peer-review under responsibility of ATI NAZIONALE

Keywords: Thermoacoustic; Instabilities; Humming

*Corresponding author. Tel.: +39-080-596-9462 ; fax: +39-080-596-3411.
E-mail address: d.laera@poliba.it

1876-6102
Selection and peer-review under responsibility of ATI NAZIONALE
doi:10.1016/j.egypro.2014.01.146

Nomenclature

a	General variable
A	Cross sectional area
c	Speed of sound
f	Frequency of oscillation
Ga	Air mass flow
GR	Growth rate
i	Imaginary unit
$\Im$m	Imaginary part
k	Acoustical wave number
l	Length
M	Mach number
p	Pressure
q	Volumetric heat release
r	Reflection coefficient
$\Re$e	Real part
t	Time
T	Transfer matrix coefficient
u	Velocity vector
x	Position vector
z	Acoustic impedance

Greek:

α	Area ratio
γ	Ratio of specific heats
λ	Eigenvalue = -i ω
κ	Interaction index
ζ	Pressure loss coefficient
ρ	Density
τ	Time delay
ω	Angular frequency
Ξ	Coupling Index

Superscript:

$\bar{\cdot}$	Mean quantity
$'$	Fluctuating quantity
$\hat{\cdot}$	Complex quantity

Subscript:

cc	Combustion chamber
l	Plenum
br	Burner
d	Downstream
eff	Effective
i	Injection location
m	Generic index
n	Generic index
red	Reduced
u	Upstream

1. Introduction

Modern gas turbine combustion chambers fuelled by natural gas suffer the problem of thermoacoustic instability. This phenomenon is due to the mutual interaction between acoustic waves and heat release oscillations of the flame. Due to propagation and reflection, the acoustic waves which develop in the flame zone invest all the combustion chamber so that the proper operation of the system may be compromised. This phenomenon is generally referred as *thermoacoustic instability*, owing to the cited coupling mechanism of pressure waves and heat release fluctuations. Often it is also referred as *humming*. It becomes dangerous when the pressure and velocity oscillations produce self-sustained vibrations which may cause fatigue cycles on system elements and blow off/flashback phenomenon of the flame. In the best case, combustion instabilities will drive a premature deterioration of components of the combustion chamber with consequent lowering of efficiency and power production. In the worst cases, failure of some components may occur with the need of rapid shut-down and interruption of the power generation.

Literature is full of works regarding different approaches to understand and analyse thermoacoustic instabilities in the gas turbine combustion chambers. Both theoretical and experimental investigations were carried out aiming at defining a method able to predict in which condition thermoacoustic instability may occur in a given combustor. These approaches can be grouped into three different categories, ordered by increasing complexity: low order acoustic models [1], acoustic models solved by Finite Elements Methods (FEM) [2], CFD (computational fluid dynamics) models [3]. Low order models are based on the idea that complex thermoacoustic systems such as in gas turbines can be represented by simple network models of lumped elements like supply duct, burner, flame, chocked exit, etc. The flame is usually regarded as a thin element characterized by the flame transfer function (FTF) [4], defined as the ratio between relative fluctuations of the heat release and relative fluctuations of the velocity at the burner exit. Both fluctuations are normalised with their respective mean values.

With the increase of the complexity of the geometry of the system, low order models may become unsuited to describe the system [5]. The acoustic phenomena can be described by the wave equation with additional terms that represent the source of pressure fluctuations produced by the flame. This equation can be solved by means of a Finite Element Method as shown in [6][7]. Unlike low order models, three-dimensional geometries can be examined. This approach solves numerically the differential equation problem converted in a quadratic complex eigenvalue problem in the frequency domain. From the complex eigenvalues of the system it is possible to ascertain if the corresponding mode is unstable or if the oscillations will decrease in time, i.e. the mode is stable. A realistic description of the flame shape can be adopted making use of CFD simulations [8][9].

CFD codes, including URANS and LES, can theoretically detect all the main effects of the phenomenon. Particularly, LES codes are proposed in order to investigate combustion instability and matching pressure oscillations with turbulent combustion phenomena, even though they require large numerical resources.

In this work, a finite element method based software is used to predict the onset of thermoacoustic instabilities of an experimental test rig.

The analysed system is designed to study the propensity to thermoacoustic instabilities of full scale industrial burners used in gas turbine system for the production of energy. So, the studied test rig is characterized by geometrical measures not comparable with the academic systems described in the literature [4] [10] [11]. It results in a series

of different modelling problems: the influence of the air feeding line and the required gas exhaust system can not be considered as negligible. So, inlet and outlet boundary conditions are not simply defined. Two different outlet boundary conditions are evaluated in order to compute the acoustic decoupling of combustion chamber.

Furthermore, due to the complexity of the geometry of some elements, such as the burner, some simplifications are needed. The Transfer Matrix approach is described and used to model these elements.

At first a purely acoustic modal analysis is carried out, i.e., no heat release fluctuation. Frequencies and wave shapes of acoustic modes of the system are studied. Subsequently, heat release fluctuation is introduced in the acoustic equation as a source term. Due to the lack of CFD data, the simplified approach of the flame sheet is used to model the flame. The sensitivity to the parameters of the Flame Transfer Function (FTF) is studied. Numerical results are compared with experimental data. The experimental work is conducted in collaboration with Ansaldo Energia and CCA (Centro Combustione e Ambiente) at the Ansaldo Caldaie facility in Gioia del Colle (Italy).

2. Mathematical Model

The following formulation is based on a new eigenmode analysis using a hybrid technique developed in Ref. [6] so the description here is kept to minimum. The interested reader can find more details in the above mentioned paper.

In presence of a linear flux with small perturbations a generic flow variable a is treated as the sum of two terms

$$a = \overline{a} + a', \tag{1}$$

where the over-bar indicates a mean quantity and the prime indicates a perturbation over the time. Moreover, the fluid is assumed as an ideal gas, viscous losses and heat conduction are neglected. Under these assumptions, applying the decomposition in Eq. (1) at each variable of the Navier-Stokes and energy equations, a set of linearised equations which describe acoustic perturbations are derived [12]. Furthermore, in gas turbine combustion chamber Mach number is generally far below unity, so the flow velocity can be regarded as negligible.

The mathematical model used to describe the thermoacoustic problem is obtained from these assumptions and based on the following inhomogeneous wave equation

$$\frac{1}{\overline{c}^2}\frac{\partial^2 p'}{\partial t^2} - \overline{\rho}\nabla\cdot\left(\frac{1}{\overline{\rho}}\nabla p'\right) = \frac{\gamma-1}{\overline{c}^2}\frac{\partial q'}{\partial t}. \tag{2}$$

where q' represents the fluctuation of the heat input per unit volume, p' is the acoustic pressure oscillation, $\overline{\rho}$ is the mean density, t and c are, respectively, time and the sound velocity. Since mean flow velocity is negligible, no entropy waves are produced in the domain.

Eq. (2) is solved in the frequency domain. In the harmonic analysis, the generic fluctuating quantity a' is written as $a' = \mathfrak{Re}(\widehat{a}\, exp(i\omega t))$, where $\widehat{a}$ is a complex quantity and ω is a complex angular frequency. Its real part gives the frequency of oscillations $f = Re(\omega)/2\pi\,[Hz]$, while its imaginary part can be used to define the growth rate (GR), an index that allows the identifications of unstable modes $GR = -\mathfrak{Im}(\omega)/2\pi\,[Hz]$. If GR is positive the acoustic mode is unstable because the amplitude of fluctuation grows exponentially with time. If GR is negative the acoustic mode is stable, i.e., perturbations decay with time.

Introducing the harmonic fluctuations, Eq. (2) becomes

$$\frac{\lambda^2}{\overline{c}^2}\widehat{p} - \overline{\rho}\nabla\cdot\left(\frac{1}{\overline{\rho}}\nabla\widehat{p}\right) = \frac{\gamma-1}{\overline{c}^2}\lambda\widehat{q}, \tag{3}$$

where $\lambda = -i\omega$. Eq. (3) is a quadratic eigenvalue problem that is solved by means of a FEM solver with an iterative linearisation procedure.

2.1. Acoustic boundary conditions

The definition of the boundary conditions is a very important step. An outlet boundary in which the chocking condition is reached is usually treated as a closed end. It means that the material derivative of the velocity fluctuations is set to be zero, $Du'/Dt = 0$. If the hypothesis of neglecting the mean velocity is applicable, the condition can be

confused with $u' = 0$. The opposite to the closed end condition is the open end. It means that the pressure fluctuation is imposed to zero, $p' = 0$.

In actual systems, to account the influence of upstream and downstream elements an acoustic impedance should be defined. In the frequency domain, the acoustic impedance is defined as

$$\widehat{z}(x,\omega) = \overline{\rho}\,\overline{c}\frac{\widehat{p}}{\widehat{u}} = \overline{\rho}\,\overline{c}\frac{1+r}{1-r}, \tag{4}$$

where x is a spatial coordinate, r is the reflection coefficient. The value of $\widehat{z}$ can be obtained experimentally by means of reflection coefficient measurements. Otherwise, literature is full of mathematical models describing different typical configurations [14].

At the boundaries where the Transfer Matrix is applied, the corresponding acoustic velocity is imposed, while continuity condition is applied to all the internal interfaces characterized by flow passage.

2.2. Transfer Matrix Method

In the transfer matrix approach an acoustic element is mathematically modelled with a system of linear equations, which is the transfer matrix. In this system the unknowns are the fluctuations of acoustic pressure p' and acoustic velocity u' at the junctions, or ports of the element. This assumption is valid under the hypothesis of unidimensional propagation of acoustic waves and if the modelled element can be treated as a compact element, i.e., its axial length is negligible compared with the wave length

$$\begin{bmatrix} \frac{\widehat{p}}{\overline{\rho}\overline{c}} \\ \widehat{u} \end{bmatrix}_d = \begin{bmatrix} T_{11} & T_{12} \\ T_{21} & T_{22} \end{bmatrix} \begin{bmatrix} \frac{\widehat{p}}{\overline{\rho}\overline{c}} \\ \widehat{u} \end{bmatrix}_u, \tag{5}$$

where subscripts u and d respectively refer to the section upstream and downstream of the element.

The coefficients T_{ij} of the transfer matrix can be obtained experimentally or numerically from CFD or aeroacoustic codes [6]. In this work the adopted transfer matrix is taken from the work of Fanaca and Alemela [4]

$$\begin{bmatrix} \frac{\widehat{p}}{\overline{\rho}\overline{c}} \\ \widehat{u} \end{bmatrix}_d = \begin{bmatrix} 1 & M_u - \alpha M_d(1+\zeta) - ikl_{eff} \\ \alpha M_u - M_d & \alpha + M_d ikl_{eff} \end{bmatrix} \begin{bmatrix} \frac{\widehat{p}}{\overline{\rho}\overline{c}} \\ \widehat{u} \end{bmatrix}_u \tag{6}$$

where $\alpha = A_u/A_d$ is the area ratio, ζ a pressure loss coefficient, which can be evaluated from the steady state incompressible Bernoulli equation [13]

$$\zeta = \frac{2\Delta p}{\overline{\rho}\,\overline{u}_d^2}, \tag{7}$$

where $\overline{u}_d^2$ is the mean flux velocity evaluated in the downstream cross section of the system.

The transfer Matrix approach is also described and used to model elements in which the low Mach number approximation can not be applied. The effective length l_{eff} is a measure of the accelerated mass in the compact element. It is defined as

$$l_{eff} = \int_{x_u}^{x_d} \frac{A_u}{A(x)}\,dx, \tag{8}$$

and it takes into account variations of the cross section.

In Eq. (6) the T_{21} element is written as a function of α, M_u and M_d. It can be also formulated as a function of the reduced length l_{red}, which is defined as $l_{red} = \int_{x_u}^{x_d} \frac{A(x)}{A_d}\,dx$.

2.2.1. Burner modelling

Burners used in gas turbine systems have a complex geometry. The examined configuration has a hybrid burner composed of multiple air and fuel lines. Air is injected through two different coaxial swirlers (diagonal and axial) with the main air mass flow passing through the diagonal passage. Fuel is injected through small holes in the vanes

of the diagonal passage. At the exit of the burner, a cylindrical volume called Cylindrical Burner Outlet (CBO) is located.

Different modelling approaches, characterized by different level of simplifications, are compared. The actual burner geometry is shown in fig. 1(a). In this full detailed model only the fuel injection holes are not considered. Due to the presence of a lot of small elements a fine computational mesh is required. This results in an heavy computational cost. Thus, in order to reduce the computational effort some simplifications are needed. First of all, the axial swirler is neglected. This means that the mass flow is considered elaborated by only the diagonal swirler. Subsequently, in order to further simplify the model, even the presence of the swirl blades is overlooked. The simplified model is showed in fig. 1(b).

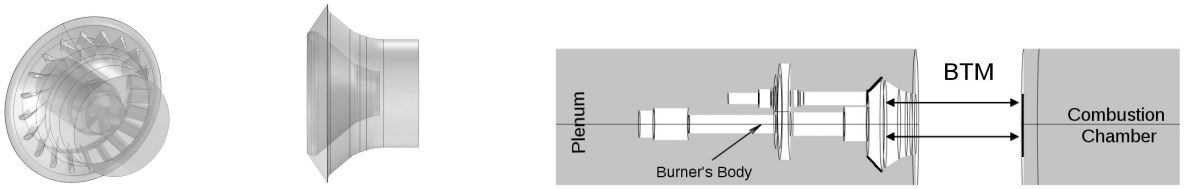

(a) Detailed Burner (b) Simplified Burner (c) Burner Transfer Matrix

Fig. 1: Burner's modelling approaches

The influence of these simplifications is studied by means of an eigenvalue analysis of a simple configuration under the hypothesis of no heat release oscillations. In this preliminary analysis the hypothesis of low Mach number approximation is considered valid in the whole acoustic domain. Furthermore, no viscous losses and heat conduction are taken into account.

A further simplification of the computational domain can be obtained using the Transfer Matrix Approach (fig. 1(c)). No experimental transfer matrix is available for the given burner, so Eq. (6) is used. In those elements in which a significant reduction of the cross section area can be observed, the mean flow velocity may become comparable with the speed of sound. Thus, the assumption of the low Mach number approximation cannot be completely appropriate. Furthermore, with the presence of the mean flux, fluid dynamic losses should also be considered. All these aspects are taken into account in the transfer matrix model. If a mass flow rate of 1.3 [kg/s] is assumed, upstream and downstream Mach number are respectively 0.063 and 0.214. The pressure drop coefficient (ζ) evaluated by means of Eq. (7) is 1.1673. l_{eff} is set to 0.45 [m], after being calculated by Eq. (8).

For this analysis a simplified computational domain is used (fig. 2). The imposed thermodynamic and geometrical parameters are summarised in tab. 1, where subscript *cc*, *p* and *br* respectively refer to combustion chamber, plenum and burner. Plenum inlet is treated as closed end ($p' = 0$). Combustion chamber outlet is assumed as open end ($p' = 0$).

Table 1: Thermodynamic and geometrical parameters

Thermodynamic parameters			Geometrical parameters		
T_u	$[K]$	700	l_p	$[mm]$	1400
T_d	$[K]$	1700	l_{cc}	$[mm]$	1500
p_u	$[bar]$	1.10	D	$[mm]$	550
p_d	$[bar]$	1.00	A_u	$[mm^2]$	67540
Δ_p	$[mbar]$	10	A_d	$[mm^2]$	35860
			l_{br}	$[mm]$	100

Table 2: Preliminary simulation: eigenvalues

Mode Number	Detailed burner model [Hz]	Simplified burner model [Hz]	BTM model [Hz]
I	43.15	43.19	-
II	147.84	147.78	146.18 + 5.86i
III	203.31	203.07	198.30 + 9.83i
IV	359.88	359.58	361.84 + 1.55i
V	417.55	417.21	418.68 + 3.35i

In tab. 2 the resonant frequencies of the first five modes obtained using different burner models are compared. Geometrical simplifications result in only small changes in the values of all resonant frequencies. So, it is possible to conclude that these simplifications have small influence on the frequencies of the modes. With the introduction of the Transfer Matrix, the first mode (bulk mode) disappears. This is caused by dissipation of the acoustic energy in the burner acoustic losses. Due to the presence of acoustic losses, the eigenvalue analysis results in a complex value.

The real part represents the resonant frequency, while the inverse of the imaginary part is the growth rate coefficient. No heat release fluctuation is considered, so all four modes results stable, i.e., negative growth rate. However, the imaginary part can still be used as an estimate of the acoustic damping of the mode.

The wave shape of the third mode in all three configurations is presented in fig. 4. Small differences appear using the transfer matrix, particularly in the neighbourhood of the minimum pressure. This is due to the acoustic damping imposed by the burner.

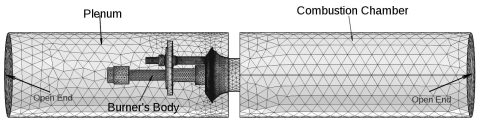

Fig. 2: Computational Domain

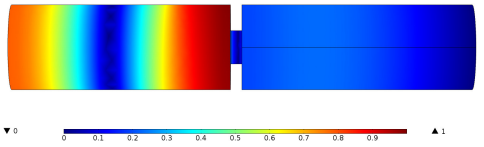

Fig. 3: Third resonant mode

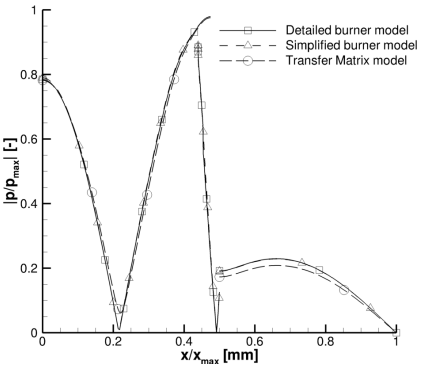

Fig. 4: Wave shapes comparison of the third resonant mode

2.3. Flame Response Function

Flame is usually regarded as a flame sheet located at the inlet of the combustion chamber. In this domain, owing to the cited coupling mechanism with pressure waves, heat release fluctuations are usually expressed as a function of acoustic variables by means of the Flame Transfer Function (FTF). According to the k-τ approach, the FTF is modelled by

$$\widehat{q} = \kappa f(\widehat{p_i}, \widehat{u_i}) exp(\lambda\tau) \tag{9}$$

where κ is the interaction index, τ is the time delay and f is a function of pressure and velocity; the subscript i denotes the injection location. Usually a linear relation between q' e u' is considered. In the frequency domain it results in

$$\frac{\widehat{q}(\mathbf{x})}{\overline{q}(\mathbf{x})} = -\kappa \frac{\widehat{u_i}\, exp(\lambda\tau)}{\overline{u}_i}. \tag{10}$$

The time delay τ is the time between the initial perturbation and the heat release fluctuations. It accounts all physical and chemical delays involved in the transport mechanism [15]. In an actual flame the time delay differs from one point to another and even from one frequency to another. In this work a mean value of τ is assumed.

3. Application

An overview of the geometry of the setup for the thermoacoustic experiments is shown in fig. 5. The atmospheric test rig developed by *Centro Combustione e Ambiente*(CCA) and *Ansaldo Energia* is characterized by two acoustic volumes, plenum and combustion chamber, coupled by the burner. The length of both chambers can be varied with continuity in order to force the instability of different frequencies. The tuning of the combustion chamber is realized by means of a mobile orifice. Variation of the geometry of the orifice results in different downstream boundary conditions. In this work, a multi-holes orifice with an equivalent diameter of 150 mm is used. Measurements of the acoustic pressure, both in the plenum volume and in the combustion chamber, are conducted by means of pressure transducers. The Multi-Microphone-Method (MMM) [1] [16] is used to reconstruct the acoustic field. This method is an extension of the well-known two microphone method [17] , which allows for a simple assessment of the measurement error by the comparison of the reconstructed acoustic field with the pressure measurements. Thermocouples allow temperature

measurements along the entire length of the combustion chamber. Air inlet temperature is driven to the desired value by a feedback system looping on the difference between its measured value and a chosen set point value. The same technique is used to manage the other input process parameters such as air and gas mass flow rate; beside this, exhaust properties (temperature, CO and NOx amount) are monitored all the tests long.

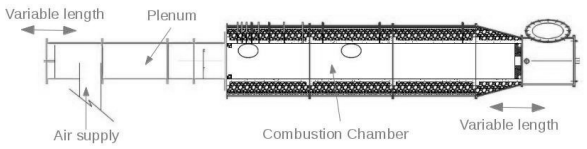

Fig. 5: Experimental setup

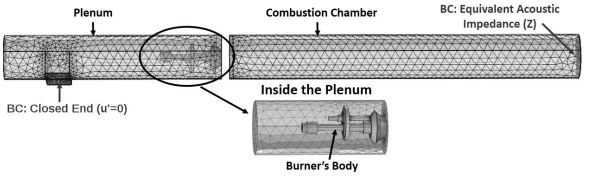

Fig. 6: Numerical domain

The test rig is characterized by a very complicated geometry so, in order to reduce the computational cost, some simplifications are introduced. The computational domain is shown in the fig. 6. In the plenum the volume occupied by the burner's body is taken into account. The combustion chamber is modelled as a cylindrical duct. The transfer matrix approach is used to model the burner. The acoustic influence of the elements downstream of the perforated orifice, in a very early stage of this analysis, is taken into account by means of an experimental acoustic impedance value.

Tab. 3 lists acoustic and thermodynamic conditions used in this study. Experimental values of temperature measured during the test are imposed in the combustion chamber. Fig. 7 shows the normalised mean temperature field. Mesh is composed of 43625 tetrahedral elements.

Table 3: Acoustic and operative conditions

T_{air}	$[K]$	523	α	[-]	1.74
Δ_p	$[mbar]$	27.83	ζ	[-]	3.62
$\overline{p}_{cc}$	$[bar]$	1.07	M_d	[-]	0.1
Ga	$[kg/s]$	1.3	M_u	[-]	0.056
l_{eff}	[m]	0.45	r_{exit}	[-]	$e^{-1.08i}$

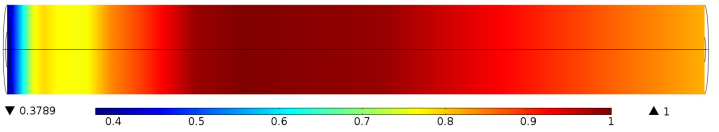

Fig. 7: Experimental normalised mean temperature field

3.1. Results

In this section results obtained in the analysis of the test rig are discussed. Although the two parts of the rig are connected each other by means of the burner, acoustic modes generally do not interest the entire system. So, it is possible to identify some regions where the normalised amplitude of a given mode is predominant and the corresponding mode is more sensitive to acoustic or geometric changes of that specific region. Only longitudinal modes will be analyse. Results will be presented in terms of normalised resonant frequency f_n and normalised growth rate g_n.

3.1.1. Acoustic modal analysis

In this preliminary phase of the analysis, no heat release fluctuation is considered. So, the RHS of Eq. 2 is null. Under such conditions, the simulation is a purely acoustic analysis whose results are the acoustic modes of the system. Different outlet boundary conditions are studied in order to verify the decoupling imposed to the combustion chamber by the multi holes orifice. Following the work of Schuller et al. [18] an acoustic coupling index can be defined as $\Xi = (\rho_d c_d)/(\rho_u c_u) A_u/A_d$. Two chambers can be fully decoupled when $\Xi \leq 0.05$, while there is weak decoupling when $0.05 < \Xi \leq 0.1$. The cross section reduction imposed by the mobile orifice results in an acoustic coupling index $\Xi = 0.0727$, which means weak decoupling. This result is confirmed by the comparison between the resonant frequencies evaluated by imposing a closed end condition and the experimental impedance value indicated in tab. 3. Tab. 4 reports the normalised resonant frequencies and, for each value, the main region in which acoustic waves propagate is indicated (Combustion Chamber CC or Plenum P). The frequency of the first resonant mode evaluated with the impedance value is used to normalised the results. It is possible to observe that only the frequencies of the

combustion chamber modes are influenced by the different outlet boundary conditions. Moreover, confirming the weak coupling, the frequency shift is few Hertz. Upstream, the burner is not able to impose a full decoupling between plenum and combustion chamber. Indeed Ξ is equal to 0.156.

First four resonant modes for the configuration with the acoustic impedance are showed in fig. 8.

Table 4: Passive simulation: eigenvalues. CC stands for Combustion Chamber and P for Plenum

Mode number	Impedance	Closed end	
	f_n	f_n	Type
I	1	1.17	CC
II	1.29	1.32	P
III	2.10	2.28	CC
IV	2.42	2.43	P
V	3.20	3.38	CC
VI	3.51	3.52	P
VII	4.31	4.50	CC
VIII	4.62	4.63	P
IX	5.43	5.62	CC
X	5.78	5.78	P

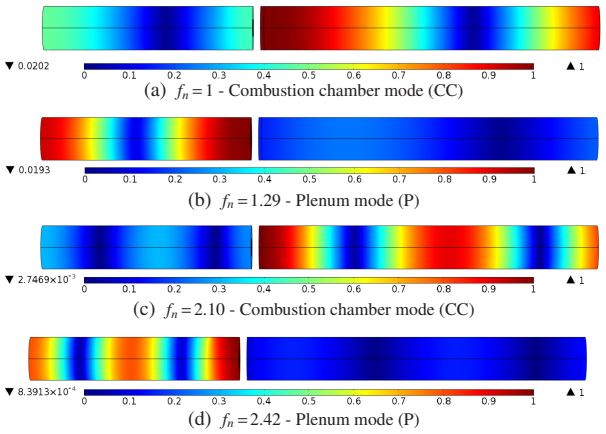

Fig. 8: First four resonant modes

It has to be clarified that when heat release fluctuation is considered, the frequency of the resonant modes may exhibit a change from the value predicted by means of the passive simulations. This is due to the presence of the FTF. So that, some frequencies predicted in this numerical analysis may not be observed in experiments. However, the simulation under passive condition is useful as a preliminary study of the influence of different operative conditions.

3.1.2. Active flame simulation

In this section heat release fluctuations are modelled in Eq. (10) as a monopole source, term $\widehat{Q} = \lambda\,\delta\,\beta\,\widehat{u}\,exp(\lambda\,\tau)$. λ is the eigenvalue, τ is the time delay, β is a non-dimensional number correlated to the intensity of the flame, δ is the reciprocal of the thickness of the flame zone. The interaction index κ in Eq. (10) is imposed to unity. In these simulations the outlet boundary condition is the complex experimental impedance value.

During the experimental tests, the system has showed instabilities around the normalise frequency 1.18. The reconstruction of the mode wave shape is carried out by means of a data fitting process. Starting from the general harmonic solution of the wave equation with mean flow in 1-D, $p'(x,t) = F\,e^{(i\,\omega\,t - i\,k_+ x)} + G\,e^{(i\,\omega\,t - i\,k_- x)}$, where F and G are respectively the amplitude of the forward travelling wave and the amplitude of the backward travelling wave. The convective wave number is defined as $k_\pm = k/(1 \pm M)$. Fixed the frequency, the wave shape, i.e. the value of F and G along the volume, is obtained minimizing the sum of square residuals between numerical values of acoustic pressure provided by the model and the ones measured during tests. For this work, four pressure trasducers are available along the combustion chamber and three in the plenum.

A good agreement between numerical and experimental results is obtained imposing $\beta = 3$ and $\tau = 3\,[ms]$ into the flame model. In these conditions, the first unstable mode, i.e. positive growth rate, is characterised by normalised frequency $f_n = 1.18$, which is equal to the one obtained during the experiments. The normalised growth rate g_n is 1.11. The numerical and experimental wave shapes of this mode in the plenum and in the combustion chamber are showed, respectively, in fig. 9(a) and fig. 9(b). The spatial coordinate is normalized with the maximum combustion chamber length.

The numerical model is able to predict the frequency and the wave shape of the resonant mode. In the plenum the comparison results not so good as in the combustion chamber. Even if the numerical model is able to predict the wave shape, an error on the position of the minimum pressure occurs. The difference is about 10 %. This may be caused by the presence of the inlet air system. In this work the plenum is modelled by a simple closed cylindrical geometry, so the influence of the air feeding line is overlooked.

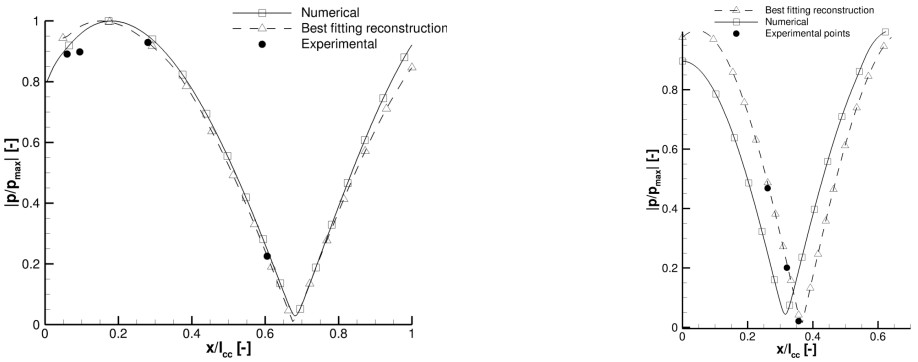

(a) Combustion chamber (b) Plenum

Fig. 9: Wave shape of the mode $f_n = 1.18$, $g_n = 1.11$

The influence of β and τ on frequency and growth rate is investigated. The first unstable mode (f_n = 1.18) is considered. Fig. 10(a) shows a periodic influence of the time delay τ with a period of 11 $[ms]$. If the time delay is increased, the acoustic mode tends to become more stable. The ratio between the time period T of the mode and the time delay τ (T/τ) tends to be non-optimal for the coupling of the acoustic of the system ad the heat release oscillations. With $\tau = 4\,[ms]$ and $\tau = 5\,[ms]$ an unstable condition is still observed, but, an increase of normalised resonant frequency up to 1.22 is showed.

The increase of the parameter β results in an increase of the normalised resonant frequency. This behaviour occurs regardless of the time delay. The nature of the normalised growth rate is not changed by the variation of β. For $\tau = 6\,[ms]$ and $\tau = 10\,[ms]$ an opposite monotone behaviour is observed.

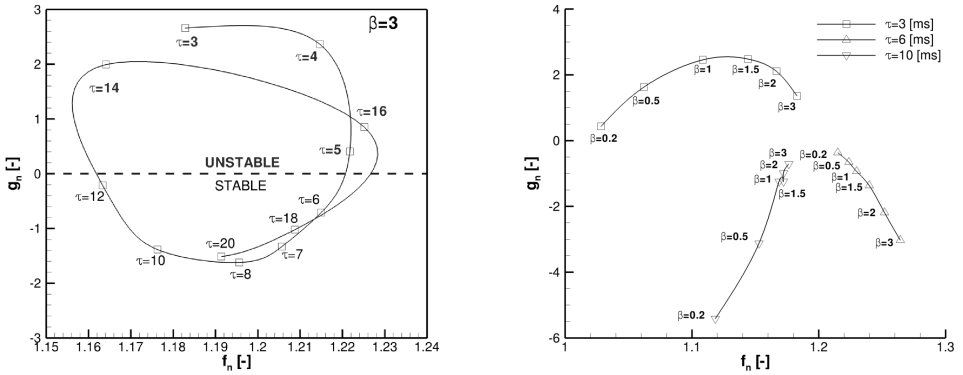

(a) Influence of time delay τ (all time delay values are in [ms]) (b) Influence of β

Fig. 10: Sensitivity to time delay τ and β

4. Conclusion

In this work a code based on the Finite Element Method able to predict the onset of thermoacoustic instabilities is applied to an experimental test rig in order to verify the ability of the method to provide a description of the phenomenon and to predict the frequency at which the instabilities occur. The experimental test is designed to evaluate the propensity to thermoacoustic instabilities of full scale Ansaldo Energia burners used in gas turbine systems for energy production.

The transfer matrix (TM) approach has been also described and used, due to the complexity of the system, to model the burner. Results confirm that the TM method is able to reproduce the acoustic influence of elements characterized by complex geometry in terms of both resonant frequencies and wave shape of the modes. Furthermore, in the Transfer Matrix acoustic and fluid dynamics losses can be taken into account.

The further ability to predict the influence of acoustic characteristics of the burner and other elements of the combustion chamber has been also verified.

Two different types of simulation are carried out under different operative conditions. At the beginning a purely acoustic analysis is conducted. The method allows the study of the acoustic resonant modes in terms of resonant frequencies and nature of the mode. Furthermore, the coupling between the combustion chamber and the downstream elements of the system is also studied. Results with two different outlet conditions, closed end and an experimental value of acoustic impedance, confirm a weak decoupling.

Subsequently, heat release fluctuations are concentrated into a narrow volume. In the combustion chamber, a good agreement between numerical and experimental results is obtained in terms of resonant frequency and wave shape of the modes. In the plenum, even if the numerical model is able to predict the wave shape of the unstable mode, an error on the position of the minimum pressure is observed. For a more accurate analysis of the plenum, measurements of the acoustic impedance of the air inlet system or an acoustically decoupling between the volume and the air feeding line are needed.

The Flame Transfer Function approach allows to study the influence of different types of flame. Frequency and growth rate of the mode result greatly influenced by the flame intensity index β and time delay τ imposed in the flame model. However, to increase the accuracy of the prediction of the influence of the Flame Transfer Function a spatial distribution of the heat release and time delay rather then the simplified flame sheet approach should be used.

References

[1] Paschereit CO, Schuermans B, Polifke W, Mattson O. Measurement of transfer matrices and source of premixed flames. J of Eng. for Gas Turbines and Power 2002; 124:239-247.

[2] Camporeale SM, Fortunato B, Campa G. A Finite Element Method for Three-Dimensional Analysis of Thermoacoustic Combustion Instability. J of Eng. for Gas Turbines and Power 2011.

[3] Martin CE, Benoit L, Sommerer Y, Nicoud F, Poinsot T. Large-Eddy simulation and acustic analysis of a swirled staged turbulent combustor. Advances in applied acoustics (AIAA) 2006; 44:741-750.

[4] Alemela PR, Fanaca D, Ettner F, Hirsch F, Sattelmayer T, Schuermans B. Flame transfer matrices of a premixed flame and a global check with modelling and experimental. GT2008-50111 in Proc. of ASME Turbo. Expo 2008, Berlin, Germany.

[5] Campa G, Camporeale S, Guaus A, Favier J, Bargiacchi M, Bottaro A, Cosatto E, Mori G. A quantitative comparison between a low order model and a 3D FEM code for study of thermoacoustic combustion instability. GT2011-45969 in Proc. of ASME Turbo. Expo 2011, Vancouver, BC, Canada.

[6] Campa G, Camporeale SM. Eigenmode analysis of the thermoacoustic combustion instabilities using a hybrid technique based on the finite element method and the transfer matrix method. Advances in Applied Acoustics (AIAAS), Vol. 1, Iss. 1, 2012.

[7] Campa G, Camporeale S. Influence of flame and burner transfer matrix on thermoacoustic instabilities. ASME Turbo. Expo 2010, Glasgow, Scotland, UK.

[8] Polifke W, Poncet A et al. Reconstruction of acoustic transfer matrix by instationary computational fluid dynamics. J. of Sound and Vibration 2001; 245:73-83.

[9] Fischer A, Hirsch C et al. Comparison of multi-microphone transfer matrix measurements with acoustic network models of swirl burners. J. of Sound and Vibration 2006; 298:73-83.

[10] Richecoeur F, Schuller T, Lamraoui A, Ducruix S. Analytical and experimental investigations of gas turbine model combustor acoustics operated at atmospheric pressure. Competes Rendus Mécanique 2013, 341:141-151.

[11] Cosic B, Moeck JP, Paschereit CO. Prediction of pressure amplitudes of self-excited thermoacoustic instabilities for a partially premixed swirl-flame. ASME Turbo. Expo 2013, San Antonio, Texas, USA.

[12] Dowling AP, Stow SR, Acoustic analysis of gas turbine combustors. J of Eng. for Gas Turbines and Power 2003.

[13] Alemela PR. Measurement and scaling of acoustic transfer matrices of premixed swirl flames. Ph.D. Thesis, TUM, Munich, 2009.

[14] Allam S, Åbom M. Experimental characterization of acoustic liners with extended reaction. 29th AIAA Aeroacoustics Conference, 2008

[15] Lieuwen TC, Yang V. Combustion instabilities in gas turbine engines: operational experience, fundamental mechanisms and modelling. Progress in Astronautics and Aeronautics 2005; 210.

[16] Jang SH. On the multiple microphone method for measuring in-duct acoustic properties in the presence of mean flow. The journal of the acoustical society of America 1998; 83(3):2429.

[17] Åbom M. Error analysis of two-microphone measurements in ducts with flow. The journal of the acoustical society of America 1998; 83(6):2429.

[18] Schuller T, Durox D, Palies P, Candel S. Acoustic decoupling of longitudinal modes in generic combustion systems. Combustion and Flame 2012; 159:1921-1931.